

# **HIGH-ENERGY TRANSIENTS**

# X-ray Bursts

*Jan van Paradijs*<sup>1,2</sup>, *Walter H.G. Lewin*<sup>3</sup>

<sup>1</sup> Astronomical Institute “Anton Pannekoek”, University of Amsterdam, and Center for High Energy Astrophysics, Kruislaan 403, 1098SJ Amsterdam, The Netherlands

<sup>2</sup> Physics Department, University of Alabama in Huntsville, Huntsville AL 35899, U.S.A.

<sup>3</sup> Center for Space Research and Department of Physics, Massachusetts Institute of Technology, 37-627, Cambridge MA 02139, U.S.A.

## 1 Introduction

An X-ray burst is a sudden increase (rise time of order seconds) of the X-ray brightness of an X-ray source, which after reaching its peak decays, generally within a minute. The sky distribution of X-ray burst sources indicates that they are galactic objects (see Fig. 1); their concentration to the direction of the galactic center tells us that they lie at typical distances of  $\sim 8$  kpc, with corresponding peak luminosities of order  $10^{38}$  erg  $s^{-1}$ . The X-ray and optical properties of the persistent emission of X-ray burst sources show that they are low-mass X-ray binaries, in which mass is transferred from a rather normal low-mass ( $< 1 M_{\odot}$ ) star to a neutron star. The persistent emission is caused by the conversion of kinetic energy of the transferred matter into heat, at a rate of  $\sim GM/R$  ( $\sim 0.1c^2$ ) per gram of accreted matter. The bursts are caused by unstable thermonuclear burning of material that has accumulated on the neutron star (‘thermonuclear flash’).

The global properties of X-ray bursts, in particular their dependence on the mass accretion rate, are fairly well understood. Different from the case of  $\gamma$ -ray bursts (see the contributions by Fishman, Hartmann and Kouveliotou to this Colloquium) the relevant question about X-ray bursts is not ‘What are they?’, but rather ‘What use are they?’. As we will argue here, X-ray bursts may provide us information on the mass and radius of a neutron star. This usefulness of X-ray bursts derives from the fact that the burst emission originates from the *surface* of the neutron star, unlike the persistent emission caused by mass accretion, of which we only know that it comes from the neutron star’s near vicinity.

In the confines of this contribution we cannot discuss the properties of X-ray bursts and their dependence on important parameters, such as mass accretion rate. For an extensive discussion of many of the issues involved we refer to the recent book ‘X-ray Binaries’ (Lewin, Van Paradijs & Van den Heuvel 1995), in particular to the chapter on X-ray bursts. A detailed discussion of the possibilities to derive the mass and radius of a neutron star from X-ray burst observations has been given by Lewin, Van Paradijs & Taam (1993).

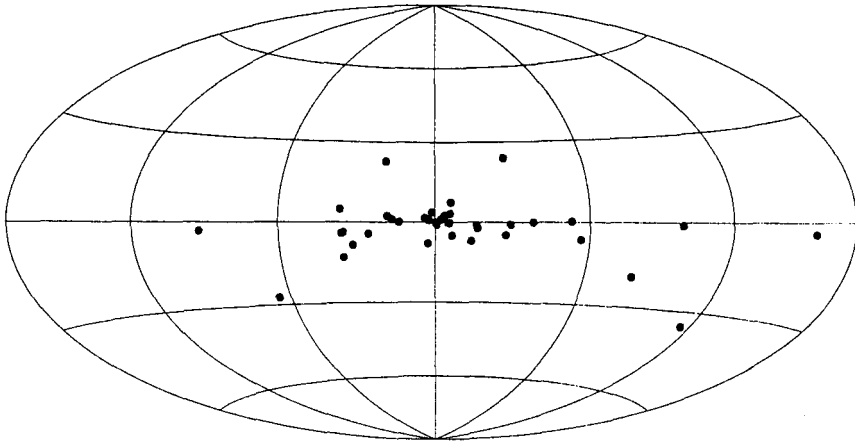


**Fig. 1.** Sky distribution of X-ray burst sources. The map is in galactic coordinates, with the equator representing the plane of the Milky Way; the origin of the map coincides with the direction to the galactic center.

## 2 Neutron star mass and radius from X-ray burst observations

A comparison of burst profiles (for the same event) as observed in different photon energy bands shows that the higher the photon energy is, the shorter is the decay part ('tail') of an X-ray burst: during the decay the X-ray burst spectrum becomes 'softer'. It was first shown by Swank et al. (1977) that burst spectra are well described by Planck functions with a temperature ( $kT$ ) varying between  $\sim 1$  and  $\sim 2.5$  keV. The blackbody interpretation was supported by the fact that during the decay the observed burst flux  $F_\infty$  (above the persistent emission) varied approximately as the fourth power of the blackbody temperature  $T_\infty$  (the subscript  $\infty$  indicates that the quantity is measured by a distant observer). This implies that during a burst one observes an approximately constant burst emitting area. For an assumed homogeneous spherical blackbody emitter of radius  $R_\infty$  at a distance  $d$ , we have

$$L_\infty = 4\pi R_\infty^2 \sigma T_\infty^4 = 4\pi d^2 F_\infty, \quad (1)$$

where  $L$  stands for luminosity. If one knew the source distance  $d$ ,  $R_\infty$  would follow from observed values of  $F_\infty$  and the associated blackbody temperatures. For a distance of 10 kpc, Swank et al. (1977) and others found radii  $R_\infty$  that are roughly compatible with those expected for neutron stars. This result forms the basis for various ways to obtain information about the mass-radius relation of neutron stars.

## 2.1 The cooling part (decay) of X-ray bursts

Because of gravitational redshift the energy of each photon emitted from the surface of a neutron star, and also the rate at which the photons arrive at a distant observer, are lower than the corresponding quantities measured at the neutron star surface, by a factor

$$1 + z_* = (1 - 2GM/R_*c^2)^{-1/2}. \quad (2)$$

Here  $M$  is the gravitational mass of the neutron star, and  $R_*$  the radius of the neutron star as observed by a local observer on its surface. As a consequence, the luminosity and blackbody temperature, as measured locally on the surface of the neutron star, are related to those measured by a distant observer as follows:

$$L_\infty = L_*(1 + z_*)^{-2} \quad (3)$$

$$T_\infty = T_*(1 + z_*)^{-1}. \quad (4)$$

Using these relations we find

$$R_\infty = R_*(1 + z_*) = R_*(1 - 2GM/R_*c^2)^{-1/2}. \quad (5)$$

These expressions are strictly valid only for non-rotating neutron stars; however, they are good approximations for neutron star spin periods larger than a few ms. The last equation shows that a measurement of  $R_\infty$  gives a relation between the mass  $M$  and radius  $R_*$  of a neutron star. It follows that  $R_\infty$  has a minimum value when  $R_* = 1.5R_g = 3GM/c^2$ ; then

$$R_{\min,\infty} = 1.5\sqrt{3}R_g \sim 7.7(M/M_\odot) \text{ km}. \quad (6)$$

For isotropic emission (such as blackbody emission) Eq. (5) does not hold when  $R_* < 1.5R_g$ : then a fraction of the emitted photons fall back to the neutron star surface, and the number of observed photons is reduced. When this is the case, Eq. (4) still holds, but Eq. (3) does not. The net result is that then

$$R_\infty = 1.5\sqrt{3}R_g \sim 7.7(M/M_\odot) \text{ km} \quad (R_g < R_* < 1.5R_g). \quad (7)$$

Since the radii  $R_*$  are likely larger than  $1.5R_g$  we do not have to be too concerned about this possibility.

In Fig. 2 we show the  $(M, R_*)$  relations for several values of  $R_\infty$ . For a given value of  $M$ ,  $R_\infty$  has a minimum; conversely, for a given observed value of  $R_\infty$ ,  $M$  cannot exceed  $(R_\infty/7.7) M_\odot$ .

In the above it has been assumed that the source distance is known, and that the radiation is emitted isotropically. Only for burst sources in some globular clusters are the distances reasonably well known. Even if the burst emission were initially isotropic it is possible that at large distances it is not, e.g., due to the presence of the inflowing matter around the neutron star. Unfortunately, our knowledge on anisotropy of X-ray emission in X-ray binaries is very poor.

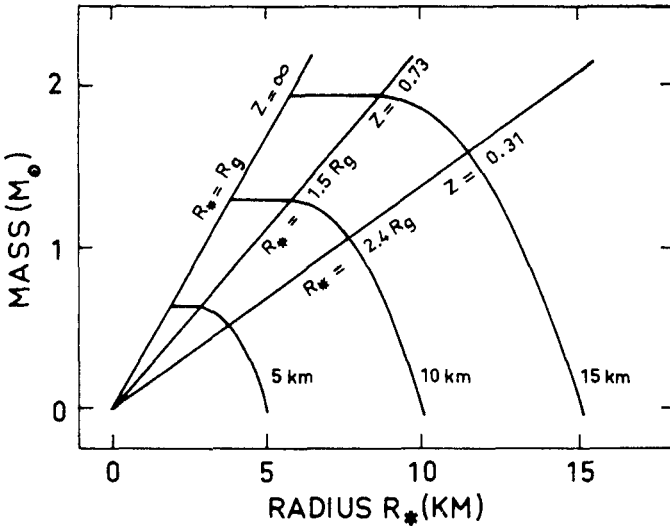


**Fig. 2.** Mass-radius relations for three hypothetical values of the blackbody radius  $R_\infty$  (5, 10, and 15 km). For clarity, we have not indicated error regions resulting from the uncertainties in the measurements. The straight lines indicate radii  $R_*$ , equal to the Schwarzschild radius  $R_g$ ,  $1.5R_g$ , and  $2.4R_g$ , respectively. The latter could, for example, be the result of a burst with radius expansion (see text), or of the determination of the gravitational redshift of an observed spectral feature. For a given mass, the observed blackbody radius,  $R_\infty$ , has a minimum value  $1.5\sqrt{3} R_g$ ; conversely, for a given blackbody radius  $R_\infty$  the mass cannot be larger than  $R_\infty/(7.7 \text{ km}) M_\odot$ .

To account for possible anisotropy one can introduce an ‘anisotropy factor’  $\xi$  according to

$$L_\infty = 4\pi R_\infty^2 \sigma T_\infty^4 = 4\pi d^2 \xi F_\infty . \tag{8}$$

To find  $R_\infty$  we need to know  $d^2\xi$ . As we discuss below, this quantity can be eliminated for bursts which show photospheric radius expansion.

### 2.2 Photospheric radius expansion

During very strong X-ray bursts the neutron star photosphere expands as a result of strong radiation pressure. Note that, different from the case of thermonuclear flashes on the surface of a white dwarf (which cause classical novae), the gravitational binding energy per gram of material is much larger than the amount of energy liberated by nuclear fusion; as a consequence only a small fraction of the accreted matter can be blown off the surface during an X-ray burst. Model calculations tell us that during the expansion, and subsequent contraction, of the photosphere the luminosity remains to within a fraction of a percent of the Eddington luminosity, at which the gravity force (directed inward) and the radiation force (directed outward) are in balance. As a result, during the expansion

the temperature of the photosphere decreases, and the spectral energy distribution shifts toward lower photon energies. This shows up as a temporary decrease of the X-ray intensity near the peak of the burst, which is particularly prominent at the higher photon energies. When the radius expansion is very large the X-ray signal may temporarily disappear altogether (the emission is then in the EUV). During the expansion and contraction phase, at photospheric radius  $R$ , the Eddington luminosity, as observed by a distant observer is

$$L_{\text{Edd},\infty} = (4\pi cGM/\kappa)(1 - 2GM/Rc^2)^{1/2} = 4\pi d^2\xi F_{\text{Edd},\infty}. \quad (9)$$

Here  $\kappa$  is the electron scattering opacity during the expansion phase (it is  $0.34 \text{ cm}^2\text{g}^{-1}$  for matter with cosmic abundances, and  $0.2 \text{ cm}^2\text{g}^{-1}$  for hydrogen-poor matter). Note that  $R$  is not  $R_*$ , but rather the radius of the photosphere which, at maximum expansion, can be many times the stellar radius. If the flux is measured during the part of the expansion when  $R \gg R_*$ , the gravitational redshift factor is unity to good approximation, and we find

$$L_{\text{Edd},\infty} = (4\pi cGM/\kappa) = 4\pi d^2\xi F_{\text{Edd},\infty} \cdot (R \gg R_*). \quad (10)$$

Just at the end of the contraction phase, when the radius of the photosphere is again  $R_*$ , the luminosity is still Eddington limited, and we have

$$L_{\text{Edd},\infty} = (4\pi cGM/\kappa)(1 - 2GM/R_*c^2)^{1/2} = 4\pi d^2\xi F_{\text{Edd},\infty}(R = R_*). \quad (11)$$

Note that  $F_{\text{Edd},\infty}$  in Eq. (10) is the observed Eddington flux when the photospheric radius is very large, whereas  $F_{\text{Edd},\infty}$  in Eq. (11) is that at 'touchdown'. A measurement of these two values of  $F_{\text{Edd},\infty}$  leads immediately to a value for  $M/R_*$  (by dividing the two equations one eliminates  $d^2\xi$ ; we assume here that the anisotropy remains constant throughout the burst). The basis of this method is shown in Fig. 3, which shows schematically the temperature versus flux diagram of a burst with radius expansion. A measurement of  $M/R_*$  limits the allowed values in the  $(M, R_*)$  diagram to a straight line through the origin.

### 2.3 Combining information from the cooling track and the radius expansion track

We can get different information about the mass and radius by combining the observations during the expansion/contraction phase (Eq. 10) with those during the cooling phase (Eq. 8); in this way we also eliminate  $d^2\xi$ . Again, this elimination is possible only if the anisotropy does not change during the burst. We then find with Eq. (5):

$$F_\infty/F_{\text{Edd},\infty} = R_*^2(1 - 2GM/R_*c^2)^{-1}\sigma T_\infty^4(\kappa/cGM). \quad (12)$$

This equation is a mass-radius relation for the neutron star, independent of the source distance and the anisotropy of the burst emission. A measurement of the

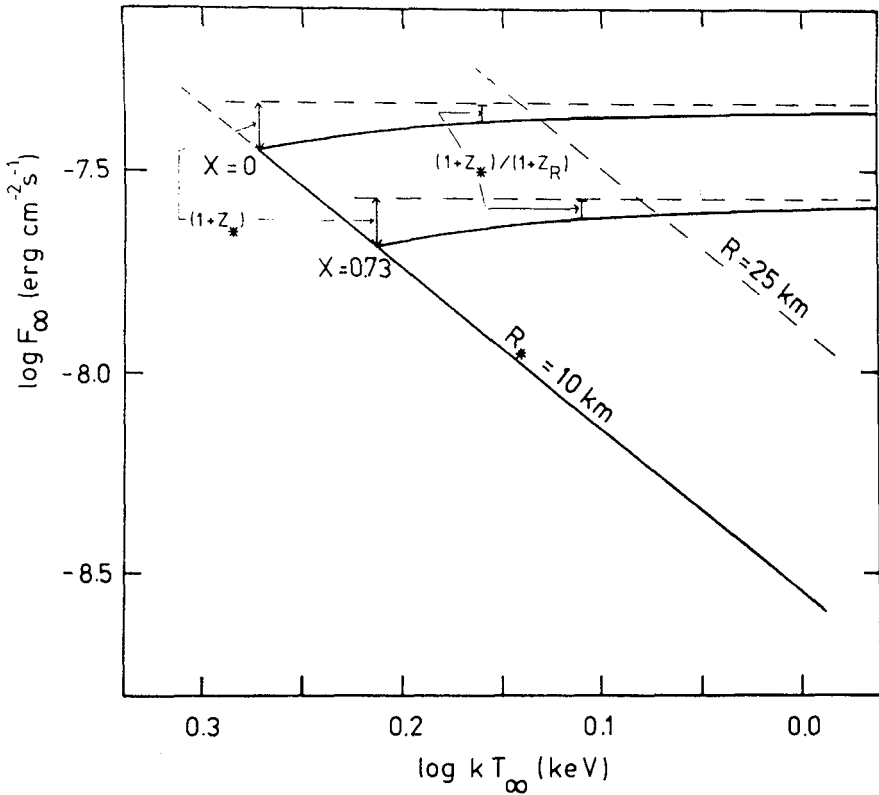


**Fig. 3.** Schematic diagram of the flux  $F_\infty$  versus the blackbody temperature  $kT_\infty$ , showing how the gravitational redshift can be determined from the variation of the Eddington luminosity during photospheric radius expansion. The straight line (cooling track) is for a sphere with constant radius; the slope of this line is 4. The slanted dashed line holds for a sphere with a 2.5 times larger radius. Two points are indicated at which the luminosity equals the Eddington limit, for cosmic (hydrogen content by number  $X = 0.73$ ) and for hydrogen-poor ( $X = 0$ ) compositions; the expansion/contraction tracks are the two solid curves. The redshift factors,  $1 + z_*$ , are indicated (assuming no change in the composition and the anisotropy).

three observables ( $F_\infty$ ,  $F_{\text{Edd},\infty}$ , and  $T_\infty$ ) then leads to a measurement of the quantity  $A = cGF_\infty / (F_{\text{Edd},\infty} \sigma T_\infty^4)$ :

$$A = R_*^2 (1 - 2GM/c^2 R_*)^{-1} (\kappa/M). \tag{13}$$

For  $R < 1.5R_g$  (see Eq. 7) the quantity  $A$  becomes:

$$A = (7.7M/M_\odot \text{ km})^2 (\kappa/M). \tag{14}$$

If  $R < 1.5R_g$ , a value of  $A$  yields a value for  $M$  which is independent of  $R_*$ . Eqs (13, 14) (in which the distance is absent) is essentially an expression for

the unchanging angular size of the burst source during the cooling phase (i.e.,  $R_\infty/d$ ). Thus, as one moves along one of the curves in Fig. 4, the angular size of the burst source remains constant, but  $R_\infty$  and  $d$  change; this is not the case for the curves in Fig. 2.

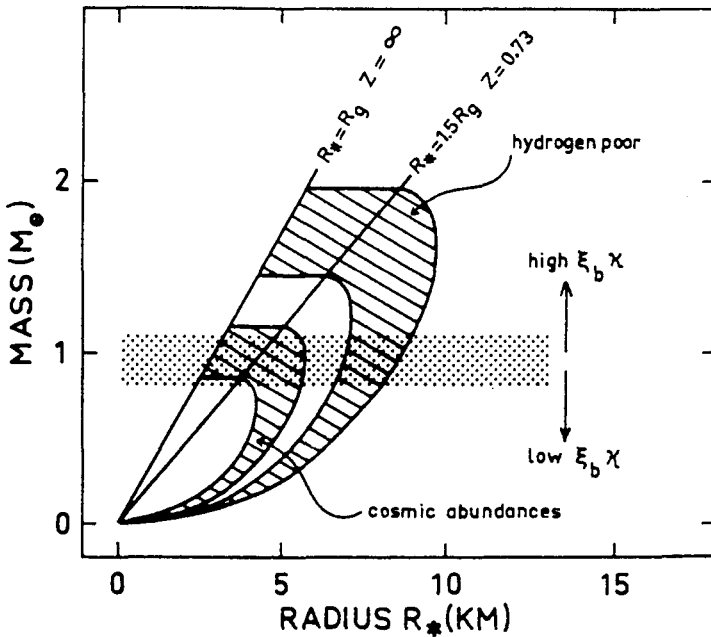


Fig. 4. Mass-radius diagram resulting from the observation of a burst with radius expansion. We have assumed, for the purpose of illustration only, that the quantity  $A$  in Eq. (13) is in the range  $(0.85-1.15)10^{-22} \text{ cm}^4 \text{ g}^{-2}$  (see text). The allowed regions in this diagram for assumed hydrogen-poor ( $\kappa = 0.2 \text{ cm}^2 \text{ g}^{-1}$ ) and cosmic ( $\kappa = 0.34 \text{ cm}^2 \text{ g}^{-1}$ ) compositions are indicated by the hatched areas. The horizontal (shaded) band indicates schematically the constraint on the mass obtained from the measured Eddington flux ( $R \gg R_*$ ) for a source with known distance. The width of the band reflects uncertainties in the measurements. The position of the band depends on both  $\kappa$  and on the anisotropy  $\xi$ , as schematically indicated.

During the decay phase of a burst with radius expansion (only one such burst per source is required), one can make several measurements of both the flux and the associated temperature. For blackbody radiation from a spherical object with a constant radius  $F_\infty/T_\infty^4$  remains constant. The average value for several measurements during burst decay can then be used to construct allowed regions in the  $(M, R_*)$  diagram. In Fig. 4 we show in the  $(M, R_*)$  diagram two curves for two values of  $\kappa$  ( $0.2$  and  $0.34 \text{ cm}^2 \text{ g}^{-1}$ ), for a typical value of  $A = 10^{-22}(\pm 15\%)$

## 2.4 Gravitational redshift from discrete spectral features

When a discrete spectral feature is present in a spectrum during times that the radiation comes from a neutron star surface, and if this feature can be identified, one has a direct measurement of the gravitational redshift at the neutron star surface, and thus of the ratio  $M/R_*$  (see Eq. 2). Lines at  $4.1 \pm 0.1$  keV have been reported in bursts from several sources. The interpretation of these absorption features is a matter of debate. A possible origin for this line is the Lyman  $\alpha$  transition in hydrogenic or helium-like iron, which would lead to  $1 + z_* \sim 1.6$ ; this would seem high, but perhaps not impossible.

## 2.5 Combining all available information

One can combine the above methods. If, in addition, the distance to the source is known [thus, the value of  $M/(\kappa\xi)$  is known (see Eq. 10)] one finds 3 equations with 4 unknowns:  $M$ ,  $R_*$ ,  $\kappa$ , and  $\xi$ . For assumed values of  $\kappa$  (e.g., hydrogen poor, or cosmic abundances) one can then, in principle, find values of  $M$ ,  $R_*$  and  $\xi$ . This analysis has been applied to the X-ray burst source 2127+119 in the globular cluster M15, for which the distance is relatively well established on the basis of optical observations of the normal stars in this cluster (see Figs. 5 and 6).

## 3 Complications

Several factors complicate the above spectral analyses of X-ray bursts in terms of neutron star mass-radius relations. For instance, the opacity  $\kappa$  is temperature dependent; it varies by about 5% over the temperature range relevant to X-ray bursts. However, this temperature dependence can be taken into account.

A much more serious effect is that the spectra emitted by hot neutron star atmospheres are not exactly Planckian. Therefore, the observed temperature that describes the shape of the spectrum ('colour temperature'  $T_c$ ) is not equal to the 'effective' temperature ( $T_{\text{eff}}$ ) used in Stefan's law (Eq. 1). In principle, modelling of the radiation transfer through the neutron star atmosphere can provide a relation between  $T_c$  and  $T_{\text{eff}}$ . Available models indicate that this is a major effect, with calculated ratios of colour temperature to effective temperature around 1.5. Moreover, observational evidence indicates that the non-Planckian character of the emitted spectrum cannot be described by just a 'hardening factor'  $T_c/T_{\text{eff}}$ . For the time being the largest uncertainty in the above ( $M$ ,  $R_*$ ) determinations is probably due to the uncertainty in this temperature conversion.

## 4 Conclusions

In the absence of any knowledge of the distance of a burst source and of the anisotropy of the burst emission, a range of allowed masses and radii of the neutron star in a given burst source can be obtained from the X-ray data of a single burst which causes radius expansion of the neutron star photosphere. If,

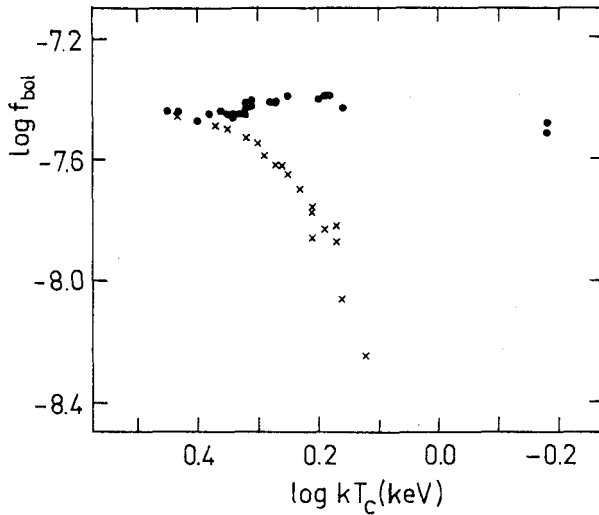


**Fig. 5.** Flux-temperature diagram for a burst with radius expansion observed from the source 2127+119 in the globular cluster M15. The dots indicate the expansion/contraction track, the crosses the cooling track. The two dots on the far right (very large radius expansion) are too low in flux; this is likely caused by the fact that only a minute fraction of the flux is sampled in the X-ray band, with a concomitant large uncertainty in the flux measurement. Notice that the cooling track is not a straight line with slope 4; this reflects deviations of the burst spectrum from a Planckian curve (Van Paradijs et al. 1990).

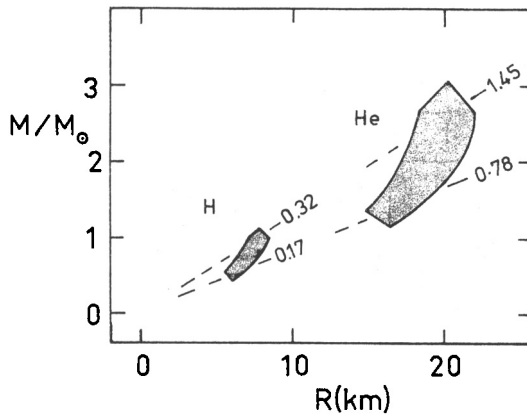


**Fig. 6.** Mass-radius diagram for the neutron star in 2127+119. The radius  $R$  in the figure is  $R_*$  as used in the text. The enclosed areas are allowed regions for assumed cosmic and hydrogen-poor compositions of the neutron star atmosphere, as indicated with 'He' and 'H', respectively. The numbers in the figure indicate the values derived for the anisotropy factors  $\xi$  (see text). (adapted from Van Paradijs et al. 1990).

in addition, the source distance and the composition of the neutron star photosphere are known, the mass and radius of the neutron star, and the anisotropy of the burst emission, can be determined separately. The largest uncertainty at present results from our incomplete knowledge of the conversion from the observed colour temperature to the effective temperature. Ongoing analysis of X-ray burst observations made with ASCA (Tanaka, private communication) may help improve our understanding of the spectra of hot neutron stars.

## References

- Lewin W.H.G., Van Paradijs J., Taam, R.E., 1993, *Space Sci. Rev.* 63, 223  
 Lewin W.H.G., Van Paradijs J., Van den Heuvel E.P.J. (eds.), 1995, *X-ray Binaries*, Cambridge University Press, Cambridge  
 Swank J.H. et al., 1977, *ApJ* 212, L73  
 Van Paradijs J., Dotani T., Tanaka Y., Tsuru T., 1990, *PASJ* 42, 633

**D.H. Hartmann:** The  $M(R)$  relationship you mentioned assumes no rotation. Do the observations support this assumption?

**J. van Paradijs:** Yes, the theoretical  $M(R)$  relation are for non-rotating neutron stars. It is generally believed that neutron stars in low-mass X-ray binaries rotate, with spin periods in the range of several milliseconds to several tens of milliseconds, due to accretion torques. However, unambiguous evidence for rotation of the low-magnetic-field neutron stars is so far lacking. The  $(M, R)$  relation would be significantly affected for spin periods below about 3 ms.

**D.H. Hartmann:** During atmosphere expansion one apparently has  $L_{\text{Edd}}(x, M) = \text{const}$ . This implies that magnetic fields in the expanding photosphere must be small. So, what do X-ray bursts tell us about magnetic field decay in neutron stars?

**J. van Paradijs:** According to current ideas the thermonuclear flash that gives rise to a X-ray burst, covers the whole neutron star surface when the mass accretion rate and the magnetic field strength of the neutron star are both relatively low. The limit on the magnetic field strength is not very strong (less equal  $10^{10} \dots 10^{11}$  G), but seems consistent with the mutual exclusion of X-ray bursts and X-ray pulsation. Somewhat in contrast: It is currently believed that the magnetic fields of neutron stars do not decay spontaneously, but that this decay is related to the accretion process – there is, however, no certainty about the details of the relation.